ADVANCED HEALTHCARE MATERIALS
www.advhealthmat.de

One-Step Photo Synthesis of Protein–Drug Nanoassemblies for Drug Delivery

Jinbing Xie, Yi Cao, Mao Xia, Xiang Gao, Meng Qin, Jiwu Wei, and Wei Wang**

In the past decade, numerous nanometer-sized drug-delivery systems (DDSs) have been developed, aiming to overcome the deficiency of conventional anticancer drugs, such as low solubility, inevitable tissue damage on extravasations, rapid in vivo breakdown, and poor selectivity for target tissues.[1–6] Among them, protein-based DDSs have recently attracted increasing attention due to their high biocompatibility, excellent biodegradability, and low toxicity.[7–12] Moreover, the high responsivity of proteins to different environmental conditions could further enhance the ability of controlled drug-release from the protein-based DDSs. An important class of protein-based nanocarriers has been derived from natural protein cages, such as viruses, ferritin/apoferritin, and small heat-shock proteins, where their original cargos (nucleic acids or iron ions) are removed and replaced by various potential drugs.[7–9] However, the number of proteins that can naturally self-assemble into such nanoscale cages is very limited. So far, many fabrication techniques have been developed to obtain protein-based DDSs, such as wet-milling, spray-freeze-drying, supercritical fluid synthesis, and microencapsulation.[13–15] These nanotechnologies are generally costly and present difficulties in producing homogeneous monodispersed nanoparticles. Self-assembly of proteins is a more convenient and cost-effective approach for protein-based DDSs. Besides naturally assembled proteins, it has been found that many proteins can self-assemble into nanoscale assemblies when they unfold or partially unfold under harsh conditions, such as low pH, high temperature, or the presence of denaturants.[16–19] Nevertheless, the tedious buffer exchange steps and the use of denaturants and organic solvents largely limit the application of these assembly methods in the preparation of DDSs; in addition, it is extremely difficult to control the morphology of such protein assemblies.

Both our group and others have recently reported that UV illumination can lead to the breakage of disulfide bonds in some disulfide-containing proteins.[20–25] We further found that the cleavage of disulfide bonds can facilitate the formation of protein nanoparticles under native conditions without the aid of any organic compounds or co-solvents.[25] Moreover, we demonstrated that it is possible to control both the shape and size of the nanoparticles by changing the intensity of UV light and the illumination time.[25,26] This approach could be developed towards the preparation of a novel DDS. Here, we report the first self-assembly approach for preparation of drug-loaded nanoparticles from disulfide-containing anticancer protein bovine α-lactalbumin (BLA) and anticancer drug doxorubicin (DOX) with uniform size distribution under physiological conditions through UV illumination. This process is one-step: drug loading and nanoparticle assembly occur simultaneously during synthesis, as shown in **Figure 1**. More importantly, the resulting protein–drug nanoparticles exhibit many desirable properties that are well suited for drug delivery: first, the BLA–DOX nanoparticles show rapid drug release at low pH and in reductive environment that are typical in tumor cells; second, the nanoparticles have synergistic anticancer activity in vitro and tumor-homing specificity in vivo, and, as a result of reducing disulfide bonds, they carry many solvent-exposed thiol groups ready for further modification and functionalization; and, third and more interestingly, the proteins in these nanoparticles are only partially unstructured – thus, many important protein functionalities (e.g., enzymatic activity or anticancer capability) can be retained in the nanoparticles.

We investigated the self-assembly process of BLA nanoparticles and their anticancer capability without the attendance of DOX. BLA is an important whey protein in cow's milk and its anticancer function is well documented in the literature.[27,28] However, the size of BLA is less than 3 nm in diameter, making it difficult to enter tumor cells directly through endocytosis.[14] Fabricating BLA nanoparticles of ca. 100 nm could improve the cell uptake of BLA and thus increase its anticancer efficiency. By illuminating the BLA solution with a concentration of 1.5 mg mL^{-1} for 5 min with a UVB lamp of 3 mW cm^{-2}, we are able to obtain uniform BLA nanoparticles of 84 ± 15 nm (**Figure 2**A). The size of the BLA assemblies can be precisely controlled by the illumination time (Figure 2B). The self-assembly mechanism of BLA is similar to that of chicken egg white lysozyme reported in our previous work.[25] First, disulfide bonds in BLA are ruptured through a tryptophan-associated photochemical process (Figure 2B). The illumination does not significantly change the secondary structures of BLA (Figure 2C) but merely induces a small alternation on the tertiary structure (Figure 2D), exposing its buried hydrophobic residues. Then, the hydrophobic interactions among these residues facilitate the self-assembly of the BLA nanoparticles. Our data also indicate

Dr. J. Xie, Prof. Y. Cao, Dr. X. Gao, Prof. M. Qin, Prof. W. Wang
National Laboratory of Solid State Microstructure and Department of Physics
Nanjing University
Nanjing 210093, PR China
E-mail: qinmeng@nju.edu.cn; wangwei@nju.edu.cn
Dr. M. Xia, Prof. J. Wei
Medical School
Nanjing University
Nanjing 210093, PR China

DOI: 10.1002/adhm.201200285

ADVANCED HEALTHCARE MATERIALS
www.advhealthmat.de

Materials Views
www.MaterialsViews.com

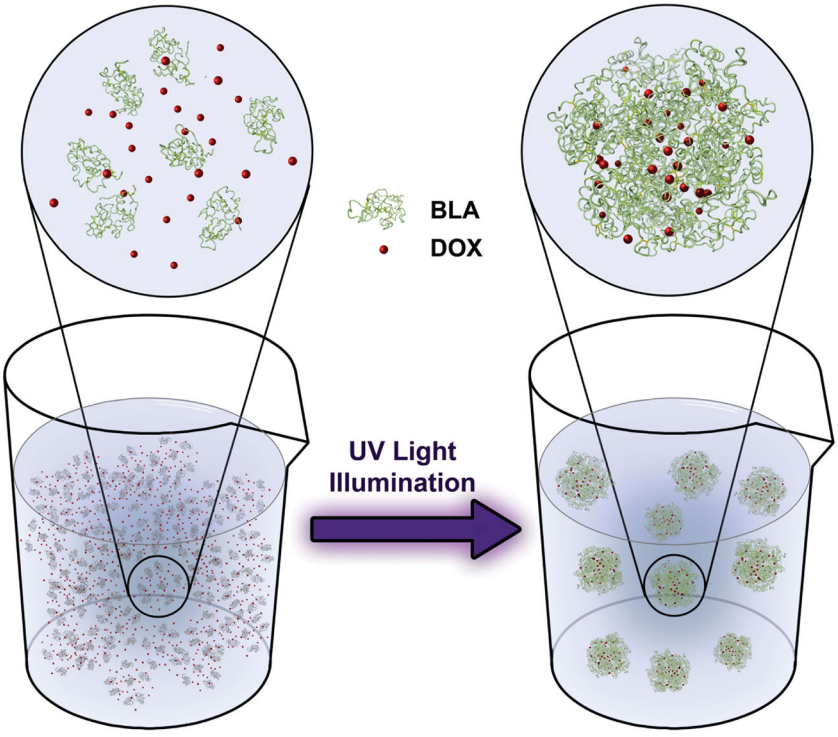

Figure 1. Schematic representation of one-step photo synthesis of protein–drug nanoparticles. Native protein BLA and drug DOX are represented as green backbone structure and red beads, respectively (left beaker), which can quickly self-assemble into BLA–DOX nanoparticles upon UV illumination through hydrophobic interaction and intermolecular disulfide bonds (highlighted in yellow).

that some intermolecular disulfide bonds are formed in the assembled BLA nanoparticles (Figure S1, Supporting Information), further stabilizing the assembled structure. As expected, formation of BLA nanoparticles can significantly improve the cytotoxicity to tumor cells. After incubation with BLA nanoparticles at a concentration of 75 μg mL^{-1} for 4 h, only ca. 40% of lung cancer cells A549 survived, while more than 80% of the cells were alive in the control experiments using unmodified BLA solution (Figure 2E). Previous studies showed that protein α-lactalbumin is biocompatible to health cell lines, such as human renal tubular epithelial cells[29] and mouse bladder epithelial cells.[28] Moreover, we showed that BLA molecules along with their assembled nanoparticles are also not toxic to the human diploid cell line derived from normal female embryonic lung tissue (WI-38), as shown in Figure 2F. Thus, the BLA nanoparticles with controllable size and morphology prepared using UV illumination are promising drug carriers.

We further developed a simple route for one-step incorporation of anticancer drug DOX into the BLA nanoparticles. For common DDSs, drug loading is often performed after the nanoparticles are prepared. However, diffusion of drugs to the center of nanoparticles requires efficient mass transfer and is often a limiting step for efficient drug loading. Moreover, organic solvents are typically required for drug loading, since most anticancer drugs are hydrophobic and insoluble in aqueous solution; this potentially increases the toxicity of the nanoparticles. We are able to eliminate this problem in producing DOX-loaded BLA nanoparticles by a simply co-assembly process of BLA and DOX. Since DOX is partially hydrophobic, it is prone to aggregation with hydrophobic residues of BLA that are exposed due to the break of disulfide bonds upon UV illumination. By controlling the concentration of BLA (1.5 mg mL^{-1}) and DOX (0.2 mg mL^{-1}) as well as the UV dose and illumination time (3 mW cm^{-2} for 5 min), we are able to obtain uniformed BLA–DOX nanoparticles of 128 ± 11.4 nm in diameter (**Figure 3**A). It is noted that little DOX is degraded during this short-time illumination process with UV light (Figure S2, Supporting Information).[30] The diameter of these BLA–DOX nanoparticles can also be easily tuned from ca. 95 to 200 nm through adjusting illumination time from 3 to 7 min (Figure S3, Supporting Information). We observed that the resulted BLA–DOX nanoparticles in the range of sub-hundred to several hundred nanometers can easily escape the capture of fixed microphages, pass through the sinusoids, and aggregate at the tumor site,[31] making them ideal DDSs. Moreover, the BLA–DOX nanoparticles prepared through this one-step method show very high package content of drugs. Herein, based on long-time dialysis (Figure S4, Supporting Information) and centrifuge-based assays, the drug-loading content and the encapsulation efficiency of the BLA–DOX nanoparticles can be determined to be ca. 70% and 8.2%, respectively, indicating good drug-carrying capability. It is worth mentioning that the exposed thiol groups resulting from disulfide bond breakage upon UV illumination make these unprotected BLA–DOX nanoparticles prone to further aggregation during storage. Meanwhile, such exposed thiol groups also provide opportunities for functionalization of polymers, such as polyethylene glycol (PEG) or targeting molecules, such as RGD peptides. Our results suggest that the PEG-modified BLA–DOX is much more stable than the ones without PEG and can be suspended in phosphate buffer saline (PBS) for several months without showing any apparent aggregation. Moreover, the PEG layer on the surface of BLA–DOX nanoparticles can avoid unwelcome drug leaking during circulation (Figure S5, Supporting Information).[32] We thus use the PEG-protected BLA–DOX for in vitro and in vivo characterization.

To check whether BLA–DOX nanoparticles can effectively release anticancer drug DOX without significant drug leaking during circulation, we monitored the in vitro release profile of DOX from BLA–DOX nanoparticles at room temperature in PBS. As shown in Figure 3B, at pH 7.4, ca. 10% of total loaded DOX was released in the first 5 h, which may correspond to the loosely bound DOX on the surface of the nanoparticles. After that, the release of DOX becomes very slow and reaches equilibrium after ca. 8 h with more than 85% of total loaded DOX still remaining in the BLA–DOX nanoparticles (Figure 3B). This suggests that the undesired release of DOX

DOI: 10.1002/adhm.201200285

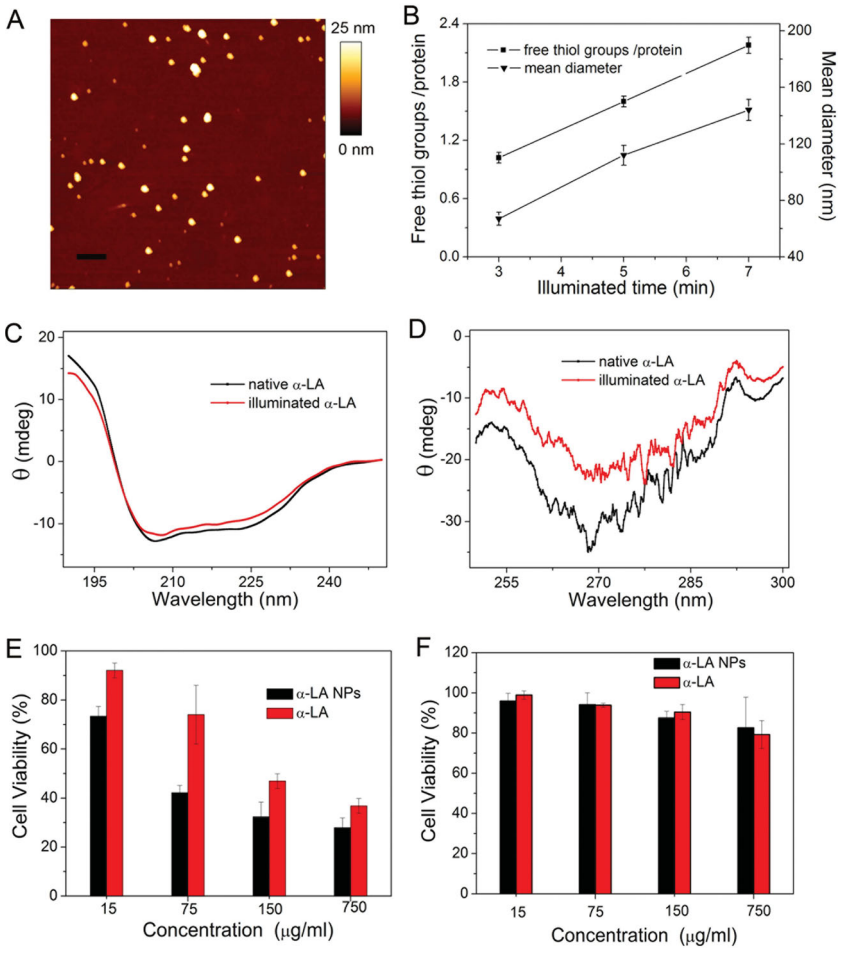

Figure 2. A) AFM image of BLA nanoparticles; the scale bar represents 500 nm. B) The number of free thiol groups per BLA molecule (left axis) measured by Ellman's reagent and the mean diameter (right axis) of BLA nanoparticles obtained by dynamic light scattering (DLS). C) Far-, and, D) near-UV circular dichroism spectra of BLA with and without 5 minutes of UV illumination. Cell viabilities of E) A549 tumor cells, and, F) WI-38 health cells after incubation with BLA molecules or nanoparticles, respectively.

during circulation can be greatly reduced. However, at ca. pH 4.0, the release rate is dramatically enhanced and more than 70% of total loaded DOX can be released from the BLA–DOX nanoparticles within 10 h. Since the microenvironment of tumor cells is exactly acidic for both the intracellular and extracellular compartments, the rapid release of DOX from BLA–DOX nanoparticles can be triggered by the acidic microenvironment of tumor cells.[33,34] As a matter of fact, the increased solubility of DOX may be the main reason of the increased drug release at lower pH (Figure S6, Supporting Information). In addition to low pH conditions, the reductive environment in tumor cells may also facilitate the release of DOX.[35,36] In the presence of 20 mM DTT, the release of DOX from BLA–DOX nanoparticles is enhanced as shown in Figure 3B. The reduction of intermolecular disulfide bonds of BLA–DOX nanoparticles is regarded to account for the enhancement. Furthermore, since both low pH and reducing environment disrupt the structure of BLA–DOX, they have synergistic effects on the release of DOX from BLA–DOX nanoparticles. At pH 4.0 and in the presence of 20 mM DTT, almost 90% of DOX in the nanoparticles can be released within 15 h. The dual response behavior makes BLA–DOX nanoparticles ideal candidates for DDSs.

We also evaluated the cytotoxicity and anticancer activity of the BLA–DOX nanoparticles. As shown in Figure 3C, the BLA–DOX nanoparticles have higher toxicity to tumor cell A549 than DOX or BLA alone. For example, the cell viability of the BLA–DOX nanoparticles (containing 250 ng mL^{-1} DOX and 3 μg mL^{-1} BLA) is ca. 48% which indicates that ca. 52% cancer cells are killed. However, the amount of cancer cells being killed under same conditions by free DOX (250 ng mL^{-1}) or protein BLA molecules (15 μg mL^{-1}) alone are only 26.83% or 5%, respectively (Figure 2E). The IC_{50} of DOX in BLA–DOX nanoparticle is ca. 250 ng mL^{-1}, which is only a quarter that of DOX alone as estimated using the Hill equation. The delivery efficiency of DOX to tumor cell A549 was also confirmed using confocal laser scanning microscopy. Under same conditions, the fluorescence intensity of DOX in the cells incubated with BLA–DOX nanoparticles is much higher than that incubated with DOX individually (Figure 3D). In fact, the fluorescence images from the red channel also yield similar results (Figure S7, Supporting Information).

To investigate whether the BLA–DOX nanoparticles can indeed target tumor tissues, we performed an in vivo experiment with mice bearing human non-small cell lung cancer A549 under their armpits and monitored tumor-targeting process by using NIR imaging. The BLA–DOX nanoparticles were conjugated with fluorescent dye NIR-797 ($BLA–DOX^{NIR-797}$) for imaging. After being injected into the tail veins of the mice, $BLA–DOX^{NIR-797}$ nanoparticles quickly diffused into the body of mice through circulation and were gradually accumulated at the tumor site probably due to the enhanced permeability and retention (EPR) effect (Figure S8, Supporting Information).[37] 48 h post-injection, the fluorescence intensity at the tumor site reached its maximum, confirmed by the mouse's fluorescent images (**Figure 4**A and B). However, as shown in Figure S8E, it is quite different for the case of BLA molecules alone that they distribute all over the body and accumulate mainly in the intestine due to the presence of abundant capillary vessels there, without the tumor homing effect. Hence, we clearly indicated that the BLA–DOX nanoparticles have great potential for drug delivery targeting tumors. Although in this study, the targeting of BLA–DOX to tumors is achieved through a passive enhanced permeability and retention (EPR) effect, we envision that our nanoparticles could be combined with ligands specific for cell surface antigens or receptors to achieve active targeting; research along this direction will be pursued as a next step.

ADVANCED HEALTHCARE MATERIALS
www.advhealthmat.de

www.MaterialsViews.com

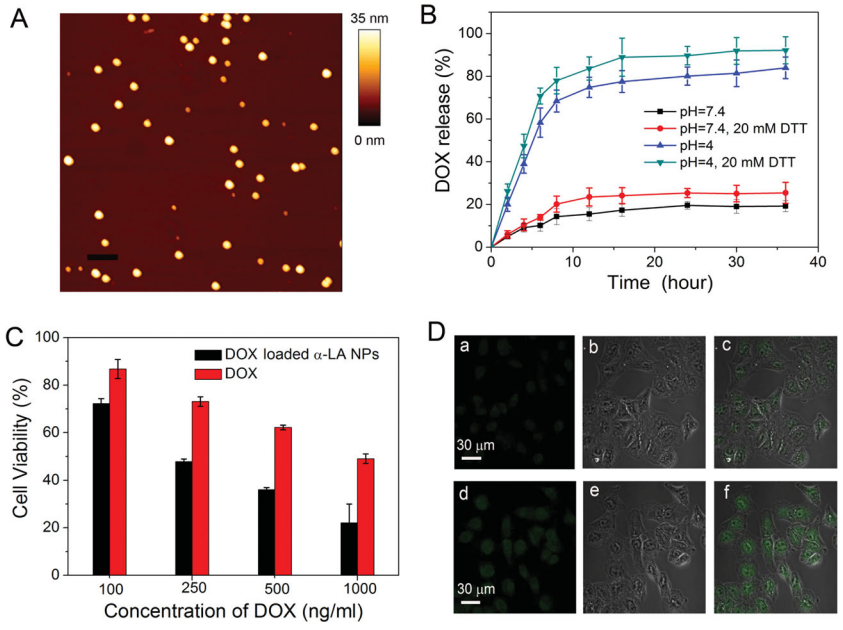

Figure 3. A) AFM image of BLA–DOX nanoparticles; the scale bar represents 500 nm. B) In vitro DOX release profiles from BLA–DOX nano-assemblies under different environmental conditions at room temperature. C) Cell viabilities of A549 tumor cells after incubation with free DOX or BLA–DOX nanoparticles of the same DOX concentration. D) Confocal laser scanning microscopy (CLSM) images of A549 tumor cells after 4 h of incubation with free DOX (a, b, c) and BLA–DOX nanoparticles (d, e, f) at 37 °C: panels a and d are obtained from the green fluorescent channel; panels b and e from the white light channel; and, panels c and f show the corresponding superimposed images.

In summary, we have introduced a novel one-step procedure to synthesize protein-based DDSs by a controlled UV illumination. A distinct advantage of this procedure is that the nanoparticle preparation and drug loading can be achieved in a single step under physiological conditions without any aid of chemical denaturants, high temperature, or organic solvents, which are likely to damage the bioactivities of drugs. The resulting protein–drug nanoparticles showed an excellent responsivity to both pH and reducing environments, enabling them suitable for application in controlled drug release. Finally, in our in vivo experiment, we demonstrated that the nanoparticles passively "homed" to the tumor site, probably through the EPR effect.

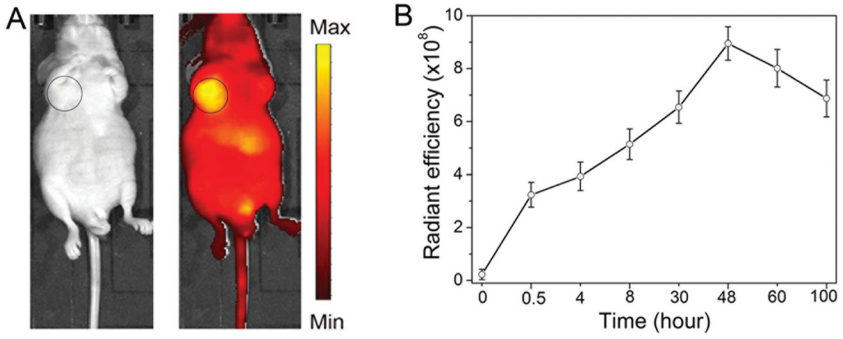

Figure 4. A) The optical (left) and NIR-797 fluorescence (right) photos of an A549 tumor-bearing mouse at 48 h after intravenous administration of BLA–DOX$^{NIR-797}$ nanoparticles. B) The NIR-797 radiant efficiency of the tumor site after in vivo administration of BLA–DOX$^{NIR-797}$ nanoparticles.

In addition to BLA–DOX nanoparticles, we expect that this methodology can also be applied to prepare protein–drug nanoparticles made of other disulfide-containing proteins and hydrophobic drugs or biomacromolecules. Moreover, it is quite feasible to conjugate active targeting motifs to the abundant free thiol groups on the surface of the nanoparticles. This novel protein-based DDS shows a promising significance for drug delivery in cancer therapy.

Experimental Section

Synthesis of the BLA and BLA–DOX Nanoparticles: 1.5 mg mL^{-1} BLA in quartz cuvettes with pathway of 1 mm was illuminated by the UV-B lamp (Philips, TL20W/12RS) with intensity ca. 3 mW cm^{-2}. For the case of BLA–DOX nanoparticles, the solution of BLA (1.5 mg mL^{-1}) and DOX (0.2 mg mL^{-1}) was illuminated for 5 min. After illumination, PEG5K-Maleimide (α-lactalbumin/PEG5K-Maleimide 1:2 w/w) was added into the illuminated solution for 60 min at room temperature. Subsequently, the solution was filtrated for 30 min under gentle agitation through a dialysis bag with a cutoff of 7000 Da molecular weight. DOX was quantified by the fluorescence intensity at 580 nm with an excitation wavelength at 480 nm.

Detection of in vitro Cytotoxicity: Here, A549 or WI-38 cells were seeded in 96-well plates and incubated with a serial concentration of assessed samples (free DOX, BLA–DOX nanoparticles) and control medium. After 48 h, 20 μL MTT solution per well was added and incubated for 4 h. The absorbance at 570 nm of each well was determined by an ELISA reader. Confocal laser scanning microscopy (CLSM) images were taken using an Olympus System Microscope BX51. A549 cells were seeded in a chamber slide and incubated for 2 d (37 °C, 5% CO_2). The medium was then replaced with 2 mL culture medium containing DOX or BLA–DOX nanoparticles, respectively. After 4 h incubation, the medium was removed and cells were rinsed once with PBS, and the slide was sealed with a microscope cover-slide and subjected to confocal microscopy.

In vitro Release of DOX from BLA–DOX Nanoparticles: This was evaluated using a dialysis bag diffusion method where 2 mL release medium (200 mL total) was periodically withdrawn and 2 mL of fresh solution was subsequently added to the system.

Detection of in vivo Tumor-homing Specificity: 2 mL BLA (10 mg mL^{-1}) and 200 mL NIR-797 (10 mg mL^{-1}) was mixed and incubated at 37 °C for 10 h with continuous stirring. The solution was dialyzed for 12 h to obtain NIR-797 labeled BLA (NIR-797-BLA), which can be used to prepare BLA–DOX nanoparticles (BLA–DOX$^{NIR-797}$ nanoparticles). Then BLA–DOX$^{NIR-797}$ nanoparticles (400 μL) were injected into A549 tumor-bearing mice (ICR, 30–32 g) through the tail vein followed by NIR fluorescence imaging using a Maestro Dynamic Lumina system (CRI, Woburn, MA). The emission wavelength was 800–900 nm and the exposure time was 2 s. Scans were carried out at 0.5, 4, 8, 30, 48, 60, and 100 h post intravenous administration. The animal experiments were performed with animal experimental permission.

DOI: 10.1002/adhm.201200285

Supporting Information

Supporting Information is available from the Wiley Online Library or from the author.

Acknowledgements

This work is supported by the National Natural Science Foundation of China under Grant Nos. 91127026, 81121062, 10904064, 11074115, 10834002 and the Priority Academic Program Development of Jiangsu Higher Education Institutions.

Received: August 15, 2012
Revised: October 26, 2012
Published online:

[1] T. M. Allen, P. R. Cullis, *Science* **2004**, *303*, 1818.
[2] A. Maham, Z. Tang, H. Wu, J. Wang, Y. Lin, *Small* **2009**, *5*, 1706.
[3] D. A. LaVan, T. McGuire, R. Langer, *Nat. Biotechnol.* **2003**, *21*, 1184.
[4] R. Duncan, *Nat. Rev. Drug Discov.* **2003**, *2*, 347.
[5] Y. Hu, Q. Chen, Y. Ding, R. Li, X. Jiang, B. Liu, *Adv. Mater.* **2009**, *21*, 3639.
[6] N. Ma, Y. Li, H. Xu, Z. Wang, X. Zhang, *J. Am. Chem. Soc.* **2010**, *132*, 442.
[7] T. Douglas, M. Young, *Science* **2006**, *312*, 873.
[8] F. C. Meldrum, V. J. Wade, D. L. Nimmo, B. R. Heywood, S. Mann, *Nature* **1991**, *349*, 684.
[9] M. L. Flenniken, D. A. Willits, S. Brumfield, M. J. Young, T. Douglas, *Nano Lett.* **2003**, *3*, 1573.
[10] F. Kratz, *J. Controlled Release* **2008**, *132*, 171.
[11] W. Lu, J. Wan, Z. She, X. Jiang, *J. Controlled Release* **2007**, *118*, 38.
[12] L. Chen, G. Remondetto, M. Rouabhia, M. Subirade, *Biomaterials* **2008**, *29*, 3750.
[13] Y. F. Maa, P. A. Nguyen, T. Sweeney, S. J. Shire, C. C. Hsu, *Pharm. Res.* **1999**, *16*, 249.
[14] M. Marsh, *Endocytosis*, Oxford University Press **2001**.
[15] K. G. Carrasquillo, J. C. Carro, A. Alejandro, D. D. Toro, K. Griebenow, *J. Pharm. Pharmacol.* **2001**, *53*, 115.
[16] C. M. Dobson, *Nature* **2003**, *426*, 884.
[17] A. D. Ferrao-Gonzales, S. O. Souto, J. L. Silva, D. Foguel, *Proc. Natl. Acad. Sci. USA* **2000**, *97*, 6445.
[18] E. N. Salgado, R. J. Radford, F. A. Tezcan, *Acc. Chem. Res.* **2010**, *43*, 661.
[19] G. Gong, F. Zhi, K. Wang, X. Tang, A. Yuan, L. Zhao, D. Ding, Y. Hu, *Nanotechnology* **2011**, *22*, 295603.
[20] M. T. Neves-Petersen, Z. Gryczynski, J. Lakowicz, P. Fojan, S. Pedersen, E. Petersen, S. Bjorn Petersen, *Protein Sci.* **2002**, *11*, 588.
[21] J. J. Prompers, C. W. Hilbers, H. A. Pepermans, *FEBS Lett.* **1999**, *456*, 409.
[22] A. Vanhooren, B. Devreese, K. Vanhee, J. Van Beeumen, I. Hanssens, *Biochemistry* **2002**, *41*, 11035.
[23] M. T. Neves-Petersen, T. Snabe, S. Klitgaard, M. Duroux, S. B. Petersen, *Protein Sci.* **2006**, *15*, 343.
[24] L.-Z. Wu, Y.-B. Sheng, J.-B. Xie, W. Wang, *J. Mol. Struct.* **2008**, *882*, 101.
[25] J. Xie, M. Qin, Y. Cao, W. Wang, *Proteins: Struct. Funct. Bioinf.* **2011**, *79*, 2505.
[26] J.-B. Xie, Y. Cao, H. Pan, M. Qin, Z.-Q. Yan, X. Xiong, W. Wang, *Proteins: Struct. Funct. Bioinf.* **2012**, *80*, 2501.
[27] M. Svensson, A. Håkansson, A.-K. Mossberg, S. Linse, C. Svanborg, *Proc. Natl. Acad. Sci. USA* **2000**, *97*, 4221.
[28] A. Håkansson, B. Zhivotovsky, S. Orrenius, H. Sabharwal, C. Svanborg, *Proc. Natl. Acad. Sci. USA* **1995**, *92*, 8064.
[29] A. Håkansson, J. Andréasson, B. Zhivotovsky, D. Karpman, S. Orrenius, C. Svanborg, *Exp. Cell Res.* **1999**, *246*, 451.
[30] K. Nawara, P. Krysinski, G. J. Blanchard, *J. Phys. Chem. A.* **2012**, *116*, 4330.
[31] J. Reichen, *News Physiol. Sci.* **1999**, *14*, 117.
[32] R. B. Greenwald, Y. H. Choe, J. McGuire, C. D. Conover, *Adv. Drug Delivery Rev.* **2003**, *55*, 217.
[33] M. Nagae, T. Hiraga, T. Yoneda, *J. Bone Miner. Metab.* **2007**, *25*, 99.
[34] J. Panyam, V. Labhasetwar, *Adv. Drug Deliv. Rev.* **2003**, *55*, 329.
[35] H. Kim, S. Kim, C. Park, H. Lee, H. J. Park, C. Kim, *Adv. Mater.* **2010**, *22*, 4280.
[36] Z. Luo, K. Cai, Y. Hu, L. Zhao, P. Liu, L. Duan, W. Yang, *Angew. Chem., Int. Ed.* **2011**, *50*, 640.
[37] H. Maeda, J. Wu, T. Sawa, Y. Matsumura, K. Hori, *J. Controlled Release* **2000**, *65*, 271.